Measurement and control of the streamer head electric field in an atmospheric pressure dielectric barrier plasma jet.

P. Olszewski[1], E. Wagenaars[2], K. McKay[1], J. W. Bradley[1] and J. L. Walsh[1*]

[1] *Department of Electrical Engineering and Electronics, University of Liverpool, L69 3BX, UK*
[2] *York Plasma Institute, Department of Physics, University of York, York YO10 5DD, UK*

Abstract

The propagation dynamics of an atmospheric pressure plasma jet resemble that of a cathode directed streamer and are determined, in part, by the localised electric field in the streamer head. This contribution employs an optical spectroscopy technique based on the polarisation dependant Stark splitting and shifting of visible helium lines to non-invasively measure the streamer head electric field. It is demonstrated that the streamer head comprises of a high field region with a peak magnitude of ~24 kV.cm^{-1} which is followed by a low field region, ~9 kV.cm^{-1}, identified as the streamer tail. The application of varying polarity voltage pulses to supplementary electrodes placed along the axis of streamer propagation was shown to influence the streamer head electric and afford a level of control over the propagation dynamics of the plasma jet, a finding that has considerable application potential.

*Corresponding author: J.L.Walsh@Liverpool.ac.uk

1. Introduction

Atmospheric pressure plasma jets provide a convenient means to deliver an abundance of highly reactive chemical species directly to a substrate; an ability that is especially useful for the processing of materials that are thermally liable or unable to withstand vacuum conditions [1]. A significant advantage of the plasma jet configuration over other atmospheric pressure plasma systems is the spatial separation between the region where plasma is generated from the region where the plasma species are applied, a characteristic that greatly contributes to the stability of the device. The transport mechanism of plasma species is highly dependent on the electrode configuration of the plasma jet and is typically driven electrically, as in the case of Dielectric Barrier Discharge (DBD) jet, or by a flowing gas, as in the case with coaxial plasma jet [2]. In the case of a DBD jet, it has been observed that the discharge takes the form of a fast moving ionisation front propagating at a velocity many orders of magnitude greater than that of the background gas flow [3]. This phenomenon, often termed a 'plasma bullet', has been the focus of intense experimental and computational investigations due to its unique physical characteristics [4]. Many studies have described the phenomenon as an ionisation front that shares many similarities to cathode directed streamers. Given that the propagation is confined to the helium-rich region exiting the jet capillary, the term 'guided streamer' was recently introduced by Boeuf *et al.* to describe the propagation process [5].

As the transport of reactive plasma species to a downstream location is of considerable practical importance, the objective of this work is to examine how the propagation dynamics, and therefore the transport of reactive plasma species, can be influenced on a nanosecond timescale. Based on the assumption that the streamer tip has a net positive charge and is therefore cathode directed [6], it is hypothesised that the application of an external electric field influences the streamer head electric field affording a level of control over the propagation dynamics. Similar techniques have been used previously to manipulate the velocity and direction of propagation [7], [8]. Indeed, it has been reported that the application of a positive voltage pulse to supplementary electrodes placed along the axis of streamer propagation leads to a reduction in propagation velocity, while a negative polarity voltage pulse leads to an increase in propagation velocity [9].

In order to evaluate the influence of an externally applied electric field on the streamer head electric field, this work employs polarisation-dependent Stark spectroscopy, a non-invasive technique with spatial and temporal resolution sufficient to characterise the electric

field profile of the streamer tip and streamer tail region. The technique, based on the splitting of visible helium emission lines was pioneered by Kuraica *et al.* and has been successfully applied to an atmospheric pressure DBD jet to obtain time-averaged electric field profiles [10][11]. Time-resolved electric fields measured using the technique are shown to agree well with those measured in previous studies and those predicted using computational models. On application of a positive voltage pulse to the external electrodes a drop in the streamer head electric field was observed, confirming the experimental and computational results reported previously by Naidis and Walsh [9].

2. Experimental Setup

The Dielectric Barrier Discharge (DBD) atmospheric pressure jet considered in this study is similar to that reported by Naidis and Walsh, and comprised of a quartz capillary 10 cm in length with a 2 mm inner diameter and 4 mm outer diameter, as shown in Figure 1. Two dielectrically covered supplementary electrodes were placed at 5 mm either side of the discharge centre line, when not energised the supplementary electrodes were held at ground potential. Helium gas was supplied at a rate of 1.75 Standard Litres per Minute (SLM) using a calibrated mass flow controller. A single copper electrode was wrapped 1 cm from the open end of the capillary and was energised using a 4.7 kV, 2.06 μs voltage pulse at a repetition rate of 7 kHz, as shown in Figure 2. Both supplementary electrodes were attached to a second pulse generator operating with a fixed pulse width of 220 ns and amplitude of ± 2 kV; the delay, Δt, between the plasma generating voltage pulse and the control pulse was varied from 200 ns to 500 ns. Electrical measurements were made using two Tektronix P6015A 75 MHz voltage probes, a Pearson 2877 200 MHz current monitor and a Tektronix DPO5054 500 MHz 4 channel oscilloscope. It is worth noting that the measured current, shown in figure 2, comprises of both the discharge current and displacement current. Subtracting the current waveform obtained with the plasma on from the current waveform obtained with the plasma off (no gas flow) effectively removes the displacement current to reveal the discharge current; however, it was found that the actual discharge current was embedded in noise generated from the high voltage pulsed power source. Following substantial filtering, discharge current pulses of 30 mA and 50 mA were obtained on the rising and falling edges of the voltage pulse respectively; such values are consistent with other studies of plasma jets operating in helium.

In order to make space and time resolved optical emission measurements the plasma jet and supplementary electrodes were mounted on a translation stage with a 25 mm travel

range in the direction of streamer propagation and 10 μm graduations. A linear polariser with an operating range of 400 - 700 nm (Thorlabs LPVISE100-A) and UV lens (UV-VIS 105 mm Coastal Optics SLR Lens) were mounted between the plasma jet and spectrometer such that a 1:1 projection of the plasma plume was made on to the entrance slit of the spectrometer which was perpendicular to the plasma jet axis. The polariser was orientated such that light from the plasma was polarised in the axial electric field direction (π–polarisation). An Andor Shamrock 500 spectrometer with 50 cm focal length, 2400 g.mm^{-1} grating and 40 μm entrance slit was used in conjunction with an Andor iStar iCCD camera to record the optical signature of the discharge with a temporal resolution down to 1.2 ns and a spatial resolution of ~40 μm. For electric field measurements, the exposure time was fixed at 10 ns and each spectrum was comprised of 560,000 individual exposures.

3. Measurement of streamer head E-Field.

In order to measure the streamer head electric field an optical technique based on the polarisation-dependent Stark splitting and shifting of visible helium lines was employed. The technique, first applied to an atmospheric pressure plasma jet by Sretenović *et al*. [11], enables the electric field to be determined based on the relative wavelength shift of the Stark sublevels of the helium 492.19 nm emission consisting of the allowed transition (1s2p $^1P_1$ – 1s4d $^1D_2$) and its forbidden counterpart (1s*2p $^1P_1$ – 1s4f $^1F_3$)*. By using a polariser with its axis parallel to the external electric field only the π components (Δm=0) of the transitions are recorded. Kuraica *et al.* show that Stark components arising from transitions between sublevels with magnetic quantum numbers m = 0 and m = 1 of both allowed and forbidden lines are unresolvable with our spectral resolution. Therefore, to evaluate the separation between the allowed and forbidden components, $\Delta\lambda_{AF}$, Kuraica *et al.* used an average value for the $m_{Upper} = 0 \rightarrow m_{Lower} = 0$ and $m_{Upper} = 1 \rightarrow m_{Lower} = 1$ displacement and fitted the results with the following third order polynomial:

$$\Delta\lambda_{AF} = 1.87.10^{-5}.E^3 + 8.8.10^{-4}.E^2 + 1.4.10^{-3}.E + 0.1316 \qquad (1)$$

Where $\Delta\lambda_{AF}$, is the separation between allowed and forbidden components in nm and E is the electric field in kV.cm^{-1} [10]. In practise, not only the E-field shifted allowed and forbidden transitions are observed, but also a field-free (ff) component originating from the area where the electric field is negligible.

Spectral lines were fitted with a pseudo-Voigt profile; figure 3(a) shows the profile of the helium (1s3p $^1P_1$ – 1s2s $^1S_0$) line at 501.57 nm, with a Full Width Half Maximum (FWHM) of 0.06 nm. Pressure (resonance) broadening is the dominant broadening mechanism under the

plasma conditions expected in this investigation, gas temperature ~320 K and an electron density of ~10^{12} cm^{-3}. Under these assumptions the FWHM resonance broadening is ~0.04 nm, while estimates for other broadening mechanisms are at least an order of magnitude smaller: Doppler broadening ~0.003 nm, van der Waals broadening ~$6x10^{-4}$ nm and Stark broadening ~$4x10^{-5}$ nm. Figure 3(b) shows a typical π–polarised spectrum of the helium 492.19 nm line from the streamer head obtained using a 10 ns exposure. A three-peak, pseudo-Voigt fit is also shown highlighting the position of the allowed, forbidden and *ff* components. From the fitted data, it is clear that the FWHM of the allowed and forbidden components is significantly wider than that of the *ff* component or the 501.57 nm profile shown in 3(a). Sretenović *et al.* present similar line profiles obtained using time-averaged spectral measurements and suggest that the broadening of the allowed and forbidden components is a consequence of the variation in E-field (from high to low) as the streamer head passes the observation point [11]. Given that the results presented in 3(b) are obtained using a short exposure (10 ns) it is surprising that the FWHM of the forbidden and allowed components do not have a comparable FWHM to the *ff* component. The broadening observed in the time-resolved measurements could indicate a lack of spatial resolution whereby both a high and low field region was observed simultaneously. Based on the simulation results of streamer head electric field presented by Naidis and Walsh it is shown that the peak electric field reduces by ~10 $kV.cm^{-1}$ within 100 μm in the wake of the streamer head [9]. Given that the spatial resolution in this investigation is ~40 μm the simultaneous observation of a high and low field region is unavoidable.

Figure 4(a) shows the temporal evolution of the Helium 492.19 nm line profile as the streamer head passed an observation point approximately 2 mm inside the quartz capillary. It is well known that the streamer head propagates at a lower velocity within the capillary (compared to when it propagates beyond the capillary) thus allowing multiple 10 ns exposures to be to be captured and the evolution of the streamer head electric field to be determined [12]. From 4(a) a clear shift of the forbidden and allowed components can be seen as the streamer head passes through the observation window. At time t = 0 ns, the electric field is found to be 23.56 $kV.cm^{-1}$ using the three-peak fitting procedure describe previously combined with eqn. 1. Within 30 ns the measured electric field had fallen to 8.81 $kV.cm^{-1}$ indicating that the streamer head had propagated beyond the observation window. Emission at t = 30 ns is likely to be from the low field region of the streamer tail. The results are in good agreement with the ~21 $kV.cm^{-1}$ presented in the earlier work of Sretenović *et al.* [11], the 23 $kV.cm^{-1}$ measured using a dielectric probe technique by Begum *et al.* [13], and

in agreement with several recent computational investigations such as Naidis [14], and Boeuf [5].

Computational studies have indicated that the electric field profile of the streamer comprises of a high field region at the tip of approximately 2 - 5 mm in length followed by a low field tail region reaching back towards the powered electrode, a rapid drop in the electric field indicates the transition from streamer tip to streamer tail [6]. In contrast to the electric field profile, the electron density is high throughout the streamer tail and rapidly decreases at the streamer tip [9]. As helium excited states are predominately populated through direct electron impact, much of the high-field region at the streamer tip is inaccessible using polarisation-dependent Stark spectroscopy due to the low electron density and subsequent low emission intensity of the helium 492.19 nm line.

As the streamer tip propagates beyond the capillary the influence of the surrounding background gas has a significant impact upon the propagation dynamics [15]. Penning ionisation between helium metastables and nitrogen impurities at the boundary layer becomes an increasingly important factor [16], and the laminar – turbulent transition of the gas flow leads to entrainment of air impurities in to the helium channel through turbulent mixing, a result of which is enhanced quenching and termination of streamer propagation [17], [18]. Figure 4(b) shows the emission profile of the helium 492.19 nm line obtained after the streamer tip had propagated beyond the observation windows. Within the capillary (0 mm) only the *ff* component is visible indicating a low electric field, as expected. Beyond the capillary (5 mm), the emission profile of the 492.19 nm line from the streamer tail indicates a low field region; however, the profile is clearly overlapping with a neighbouring nitrogen emission band. Due to this overlap and an increased velocity of propagation, the electric field measurements of the streamer tip beyond the capillary were limited to a single 10 ns exposure. Also shown in figure 4(b) is a simulated spectra of the nitrogen second positive emission band from which the rotational temperature was found to be 320 K ± 20 K, under atmospheric pressure conditions the rotational temperature and gas temperatures are known to be close to equilibrium [19].

4. Control of streamer head E-Field.

The application of an external electric field through the region in which the streamer head propagates has been shown to afford a considerable level of control over the streamer dynamics including both the direction and velocity of propagation, [7],[9],[20]. From an application perspective, the ability to electrically manipulate the streamer dynamics on a

nanosecond timescale and consequently influence the flux of reactive species arriving at a downstream has significant advantages over existing techniques. Simulation results presented by Naidis *et al.* indicate that the application of a positive voltage pulse to a downstream electrode results in a drop in the streamer head electric field and consequently a decrease in propagation velocity; conversely, application of a negative pulse to a downstream electrode results in an increase in streamer head electric field and increase in propagation velocity [9]. In this investigation ± 2 kV, 220 ns voltage pulses are applied to the external electrodes and the peak streamer head electric field determined as described in section 3.

With the external electrodes held at ground potential, a plasma plume was seen to extend approximately 2 cm beyond the exit of the capillary. The first observation point, 0 mm, was located approximately 2 mm inside the capillary and the final observation point was located 8 mm from the capillary exit. Optical measurements made >8 mm from the capillary exit were dominated by nitrogen emission making it considerably more complex to accurately determine the position of the forbidden component. Figure 5(a) shows the peak streamer head electric field with the external electrodes held at ground potential and when raised to +2 kV. Interestingly, with the external electrodes held at ground potential the peak streamer head electric field is seen to gradually decrease once beyond the capillary. Several previous studies have demonstrated that the streamer propagation velocity increases significantly as the streamer head exits the capillary [9]. The increase in velocity coupled with an unexpected decrease in streamer head electric field indicates that a complex interaction of many factors such as the streamer head radius, streamer head charge density and the level of impurity entrained in the feed gas play a role in determining the propagation dynamics. From iCCD images (not shown) it is clear that the streamer head radius varies along the axis of propagation, reaching a maximum close to the capillary exit; this increase in volume corresponds with the reduction in streamer head propagation velocity. A similar correlation between streamer radius, propagation velocity and electric field has been reported in studies focusing on positive streamers in air [21].

Application of a 220 ns positive voltage pulse approximately 200 ns after the rising edge of the plasma generating voltage pulse is seen to decrease the peak streamer head electric field by ~ 6 $kV.cm^{-1}$, it is hypothesised that this reduction is primarily responsible for the significant decrease in propagation velocity observed by Naidis and Walsh under very similar experimental conditions [9]. When the delay between the plasma generating voltage pulse

and the control voltage pulse, Δt, is varied from 200 ns to 500 ns, it can be seen that the position whereby the peak electric field decreases is shifted in space (and therefore time) demonstrating an ability to manipulate the streamer head electric field on a nanosecond timescale. Figure 5(b) highlights the impact of applying a 220 ns negative voltage pulse at a Δt of 200 ns and 500 ns; a clear increase in the peak streamer head electric field of ~5 – 7 kV.cm^{-1} is observed depending on the time of application of the control pulse relative to the position of the streamer front. Given that the propagation dynamics of a DBD plasma jet are reported to be similar to that of a cathode directed streamer it is reasonable to assume that the application of a negative voltage pulse to a closely located electrode significantly enhances the localised electric field of the positively charged streamer tip leading to an increased propagation velocity (whilst maintaining a fixed streamer head radius). From Figure 5(a) and 5(b) it can be concluded that application of a voltage pulse to external electrodes placed along the axis of propagation enables the manipulation of the streamer head electric and is therefore a viable means to electrically control the propagation dynamics of the plasma jet with high temporal resolution.

5. Summary

This paper employs a polarisation-dependant Stark spectroscopy technique to measure the electric field of a cathode directed guided streamer produced by a DBD plasma jet. It is shown that the streamer tip comprises of a high field region which rapidly propagates beyond the observation point and is followed by a low field tail region, a structure that is highly representative of a cathode directed streamer. The measurements are in qualitative agreement with several recent experimental and computational studies. As the streamer head exits the capillary, an unexpected drop in the peak electric field is observed and is attributed to the varying physical characteristics of the streamer tip. Application of nanosecond duration voltage pulses to electrodes situated along the axis of streamer propagation is shown to yield and increase or decrease of the streamer head electric field that is dependent on the polarity, magnitude and time of the applied voltage relative to the plasma generating voltage pulse. In conclusion, this contribution has highlighted the potential of externally applied electric fields to manipulate the propagation dynamics of the plasma jet through the control of the streamer head electric field; a finding that has considerable application potential.

6. References

[1] Tendero C, Tixier C, Tristant P, Desmaison J, Leprince P, 'Atmospheric pressure plasmas: A review' *Spectrochimica Acta Part B*, 61, 2 – 30, 2006.

[2] J. L. Walsh and M. G. Kong, "Contrasting characteristics of linear-field and cross-field atmospheric plasma jets," Applied Physics Letters, vol. 93, no. 11, p. 111501, 2008.

[3] M. Teschke, J. Kedzierski, D. Korzec, and J. Engemann, "High-Speed Photographs of a Dielectric Barrier Atmospheric Pressure Plasma Jet," *IEEE Transactions on Plasma Science*, vol. 33, no. 2, pp. 310–311, 2005.

[4] X. Lu, M. Laroussi, and V. Puech, "On atmospheric-pressure non-equilibrium plasma jets and plasma bullets," *Plasma Sources Science and Technology*, vol. 21, no. 3, p. 034005, Jun. 2012.

[5] J.-P. Boeuf, L. L. Yang, and L. C. Pitchford, "Dynamics of a guided streamer ('plasma bullet') in a helium jet in air at atmospheric pressure," *Journal of Physics D: Applied Physics*, vol. 46, no. 1, p. 015201, Jan. 2013.

[6] G. V. Naidis, "Modeling of helium plasma jets emerged into ambient air: Influence of applied voltage, jet radius, and helium flow velocity on plasma jet characteristics," *Journal of Applied Physics*, vol. 112, no. 10, p. 103304, 2012.

[7] J. L. Walsh, P. Olszewski, and J. W. Bradley, "The manipulation of atmospheric pressure dielectric barrier plasma jets," *Plasma Sources Science and Technology*, vol. 21, no. 3, p. 034007, Jun. 2012.

[8] A. Shashurin, M. N. Shneider, and M. Keidar, "Measurements of streamer head potential and conductivity of streamer column in cold nonequilibrium atmospheric plasmas," *Plasma Sources Science and Technology*, vol. 21, no. 3, p. 034006, Jun. 2012.

[9] G. V Naidis and J. L. Walsh, "The effects of an external electric field on the dynamics of cold plasma jets—experimental and computational studies," Journal of Physics D: Applied Physics, vol. 46, no. 9, p. 095203, Mar. 2013.

[10] M. M. Kuraica and N. Konjević, "Electric field measurement in the cathode fall region of a glow discharge in helium," *Applied Physics Letters*, vol. 70, no. 12, p. 1521, 1997.

[11] G. B. Sretenović, I. B. Krstić, V. V. Kovačević, B. M. Obradović, and M. M. Kuraica, "Spectroscopic measurement of electric field in atmospheric-pressure plasma jet operating in bullet mode," *Applied Physics Letters*, vol. 99, no. 16, p. 161502, 2011.

[12] J. Shi, F. Zhong, J. Zhang, D. W. Liu, M. G. Kong, J. Shi, F. Zhong, and J. Zhang, "A hypersonic plasma bullet train traveling in an atmospheric dielectric- barrier discharge jet A hypersonic plasma bullet train traveling in an atmospheric dielectric-barrier discharge jet," vol. 013504, 2008.

[13] A. Begum, M. Laroussi, and M. R. Pervez, "Atmospheric pressure He-air plasma jet: Breakdown process and propagation phenomenon," *AIP Advances*, vol. 3, no. 6, p. 062117, 2013.

[14] G. V Naidis, "Simulation of interaction between two counter-propagating streamers," *Plasma Sources Science and Technology*, vol. 21, no. 3, p. 034003, Jun. 2012.

[15] M. A. Akman and M. Laroussi, "Insights Into Sustaining a Plasma Jet : Boundary Layer Requirement," vol. 41, no. 4, pp. 839–842, 2013.

[16] Q. Li, X.-M. Zhu, J.-T. Li, and Y.-K. Pu, "Role of metastable atoms in the propagation of atmospheric pressure dielectric barrier discharge jets," *Journal of Applied Physics*, vol. 107, no. 4, p. 043304, 2010.
[17] M. Ghasemi, P. Olszewski, J. W. Bradley, and J. L. Walsh, "Interaction of multiple plasma plumes in an atmospheric pressure plasma jet array," *Journal of Physics D: Applied Physics*, vol. 46, no. 5, p. 052001, Feb. 2013.
[18] R. Xiong, Q. Xiong, A. Y. Nikiforov, P. Vanraes, and C. Leys, "Influence of helium mole fraction distribution on the properties of cold atmospheric pressure helium plasma jets," *Journal of Applied Physics*, vol. 112, no. 3, p. 033305, 2012.
[19] T. Verreycken, a F. H. van Gessel, a Pageau, and P. Bruggeman, "Validation of gas temperature measurements by OES in an atmospheric air glow discharge with water electrode using Rayleigh scattering," *Plasma Sources Science and Technology*, vol. 20, no. 2, p. 024002, Apr. 2011.
[20] N. Mericam-Bourdet, M. Laroussi, a Begum, and E. Karakas, "Experimental investigations of plasma bullets," *Journal of Physics D: Applied Physics*, vol. 42, no. 5, p. 055207, Mar. 2009.
[21] A. Luque, V. Ratushnaya, and U. Ebert, "Positive and negative streamers in ambient air: modelling evolution and velocities," *Journal of Physics D: Applied Physics*, vol. 41, no. 23, p. 234005, Dec. 2008.

Figure Caption:

Figure 1: Diagram of experimental setup showing plasma jet, external electrodes placed parallel to axis of propagation and optical arrangement used for measurement of streamer head E-Field.

Figure 2: Voltage waveforms of generation and control pulse. Δt denotes the delay between generation pulse and application of a control pulse to parallel electrodes.

Figure 3: (a) Line profile of Helium emission (1s3p $^1P_1$ – 1s2s $^1S_0$) at 501.57 nm and Voigt fit with 0.06 nm Full Width Half Maximum (FWHM). (b) π–polarised spectra of Helium emission at 492.19nm, showing field free (*ff*), allowed (1s2p $^1P_1$ – 1s4d $^1D_2$) and forbidden (1s*2p* $^1P_1$ – *1s4f* $^1F_3$*)* components.

Figure 4: (a) 492.19 nm Helium line profile originating from the streamer head obtained at 10 ns intervals as streamer front passes spectrometer entrance slit. Electric field values calculated using Eqn. 1. (b) 492.19 nm Helium line profile obtained from the streamer tail inside the capillary (0 mm) and beyond the capillary (5 mm).

Figure 5: Impact on peak streamer head E-Field with the application of (a) positive control pulses at 200 ns and 500 ns, and (b) negative control pulses at 200 ns and 500 ns.

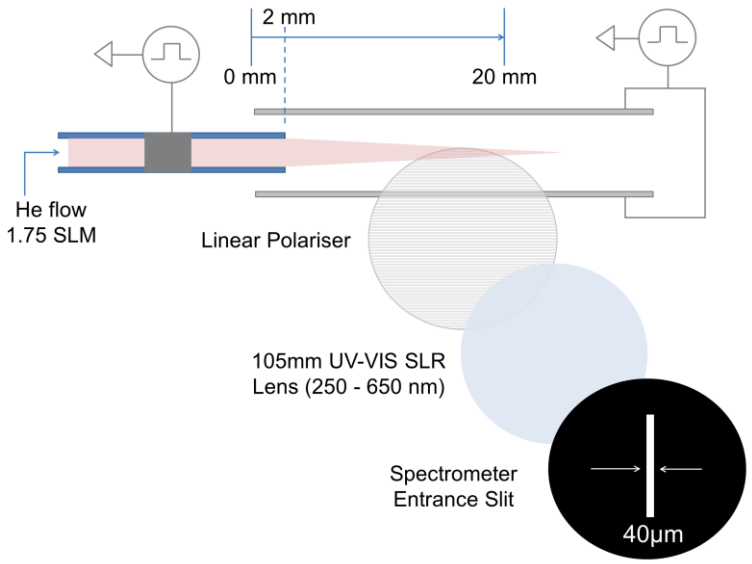

Figure 1: Diagram of experimental setup showing plasma jet, external electrodes placed parallel to axis of propagation and optical arrangement used for measurement of streamer head E-Field.

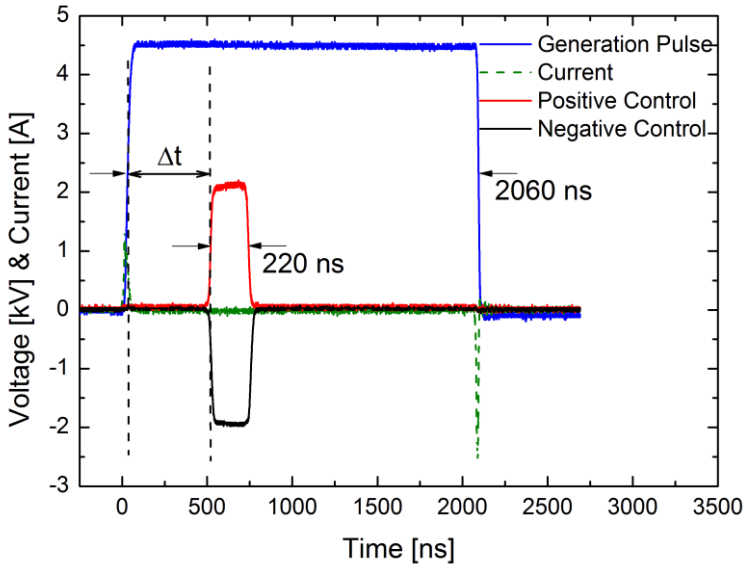

Figure 2: Voltage waveforms of generation and control pulse. *Δt* denotes the delay between generation pulse and application of a control pulse to parallel electrodes.

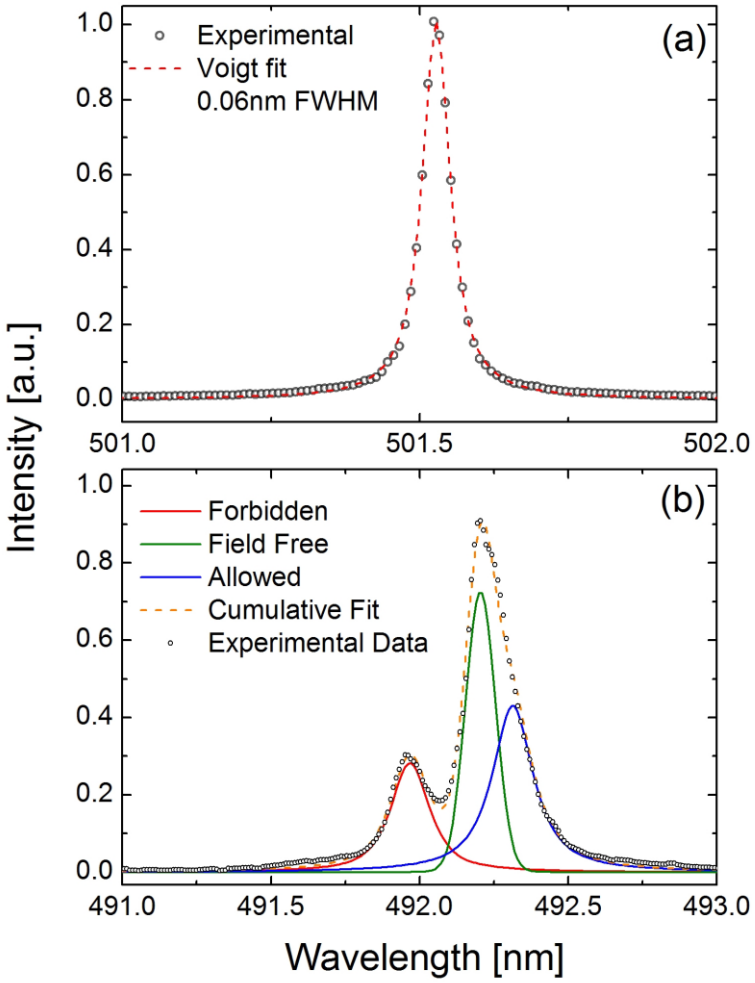

Figure 3: (a) Line profile of Helium emission (1s3p $^1P_1$ – 1s2s $^1S_0$) at 501.57 nm and Voigt fit with 0.06 nm Full Width Half Maximum (FWHM). (b) π–polarised spectra of Helium emission at 492.19nm, showing field free (*ff*), allowed (1s2p $^1P_1$ – 1s4d $^1D_2$) and forbidden (1s*2p* $^1P_1$ – *1s4f* $^1F_3$) components.

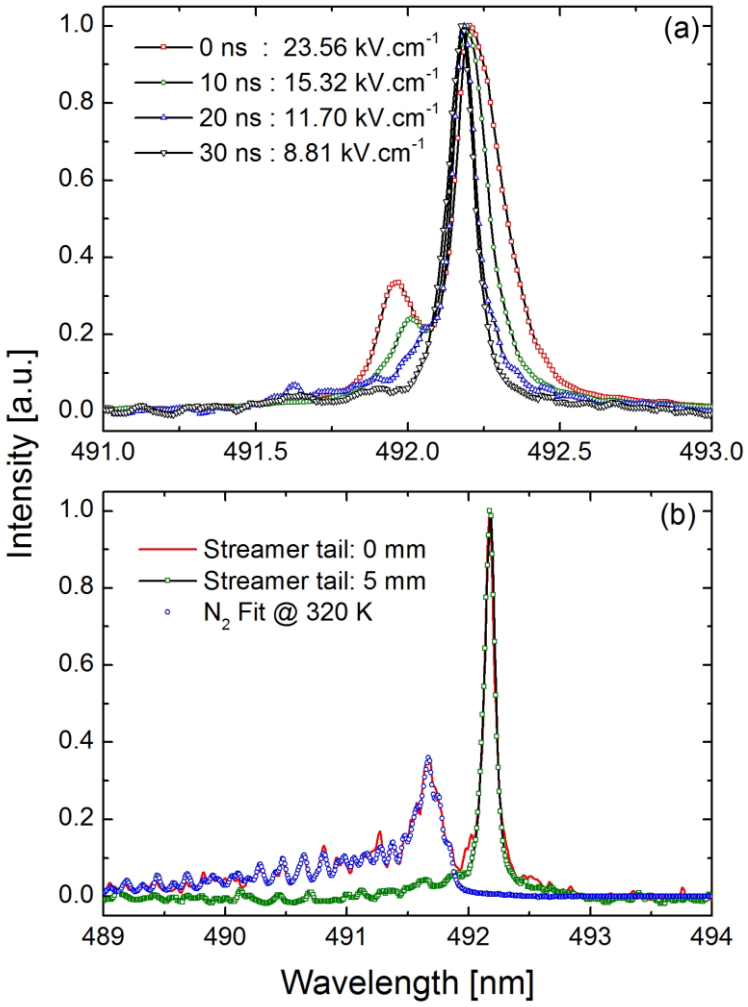

Figure 4: (a) 492.19 nm Helium line profile originating from the streamer head obtained at 10 ns intervals as streamer front passes spectrometer entrance slit. Electric field values calculated using Eqn. 1. (b) 492.19 nm Helium line profile obtained from the streamer tail inside the capillary (0 mm) and beyond the capillary (5 mm).

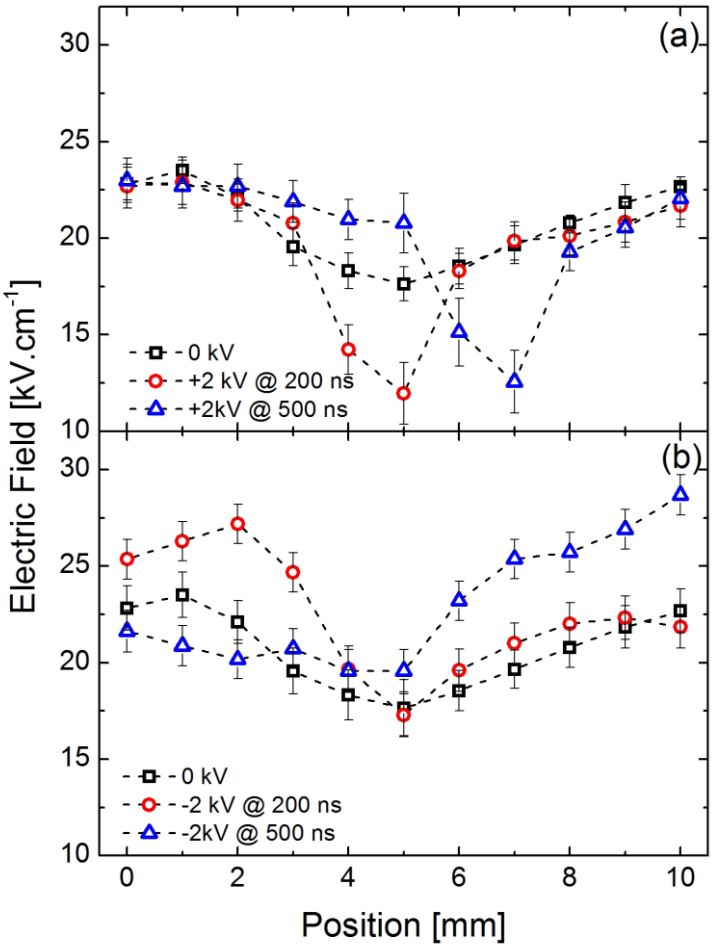

Figure 5: Impact on peak streamer head E-Field with the application of (a) positive control pulses at 200 ns and 500 ns, and (b) negative control pulses at 200 ns and 500 ns.